International Journal of Nanomedicine

Dovepress
open access to scientific and medical research

Open Access Full Text Article

ORIGINAL RESEARCH

Zerumbone-loaded nanostructured lipid carrier induces G2/M cell cycle arrest and apoptosis via mitochondrial pathway in a human lymphoblastic leukemia cell line

Heshu Sulaiman Rahman[1–3]
Abdullah Rasedee[1,2]
Ahmad Bustamam Abdul[2,4]
Nazariah Allaudin Zeenathul[1,2]
Hemn Hassan Othman[1,3]
Swee Keong Yeap[2]
Chee Wun How[2]
Wan Abd Ghani Wan Nor Hafiza[4,5]

[1]Faculty of Veterinary Medicine, [2]Institute of Bioscience, Universiti Putra Malaysia, Selangor, Malaysia; [3]Faculty of Veterinary Medicine, University of Sulaimanyah, Sulaimanyah City, Kurdistan Region, Northern Iraq; [4]Faculty of Medicine and Health Science, Universiti Putra Malaysia, Selangor, Malaysia; [5]College of Medical Laboratory Technology, Institute for Medical Research, Kuala Lumpur, Malaysia

Correspondence: Abdullah Rasedee or Heshu Sulaiman Rahman
Department of Microbiology and Pathology, Faculty of Veterinary Medicine, Universiti Putra Malaysia, 43400 UPM Serdang, Selangor, Malaysia
Tel +60 3 8946 3455
Fax +60 3 8946 1071
Email rasedee@gmail.com or heshusr77@gmail.com

Abstract: This investigation evaluated the antileukemia properties of a zerumbone (ZER)-loaded nanostructured lipid carrier (NLC) prepared by hot high-pressure homogenization techniques in an acute human lymphoblastic leukemia (Jurkat) cell line in vitro. The apoptogenic effect of the ZER-NLC on Jurkat cells was determined by fluorescent and electron microscopy, Annexin V-fluorescein isothiocyanate, Tdt-mediated dUTP nick-end labeling assay, cell cycle analysis, and caspase activity. An MTT (3-(4,5-dimethylthiazol-2-yl)-2,5 diphenyltetrazolium bromide) assay showed that ZER-NLC did not have adverse effects on normal human peripheral blood mononuclear cells. ZER-NLC arrested the Jurkat cells at G2/M phase with inactivation of cyclin B1 protein. The study also showed that the antiproliferative effect of ZER-NLC on Jurkat cells is through the intrinsic apoptotic pathway via activation of caspase-3 and caspase-9, release of cytochrome c from the mitochondria into the cytosol, and subsequent cleavage of poly (adenosine diphosphate-ribose) polymerase (PARP). These findings show that the ZER-NLC is a potentially useful treatment for acute lymphoblastic leukemia in humans.

Keywords: zerumbone-loaded nanostructured lipid carrier, cell cycle arrest, apoptosis, mitochondrial pathway

Introduction

The number of drug candidates has been steadily increasing over the last two decades. Many of these drugs, although showing great therapeutic potential, are plagued by poor solubility and consequently poor absorption, bioavailability, and delivery to target tissues and organs. Solubilization of poorly soluble drugs is limited by drug properties, chemistry, solubility in organic media, and molecular size.[1]

Many approaches have been adopted over the years to increase drug solubility, including use of surfactants, complex formation to include cyclodextrins and macromolecules, microemulsions, and micronization of drug powders to increase surface area and stability, but dissolution velocity remains insufficient to overcome the poor bioavailability of these drugs and to meet biopharmaceutical specifications.[2] Therefore, there is an increasing need to develop new pharmaceutical carriers and delivery systems that could be used to improve the efficacy of these drugs. Generally, carrier schemes for drug delivery should be nontoxic, have adequate drug-loading capacity, the possibility of targeting, and have controlled release characteristics. To maximize the usefulness of the delivery system, the incorporated drug should be chemically and physically stable with potential for scaling up at reasonable overall cost.[3]

submit your manuscript | www.dovepress.com
Dovepress
http://dx.doi.org/10.2147/IJN.S54346

Colloidal drug carrier systems have received great attention as potential drug delivery systems because they offer many advantages, including increased dissolution velocity that also leads to increased bioavailability and saturation solubility.[4] These systems may be achieved by reducing the size of particles to the nanosize range, which will increase the surface area. These nanoparticles are solid colloidal particles with sizes ranging from 1 to 1,000 nm.[5]

The solid lipid nanoparticle (SLN) is a colloidal drug carrier system that was developed as an alternative carrier scheme to existing traditional carrier systems, such as liposomes, micelles, and polymeric nanoparticles. Although the SLN has numerous advantages that include targeted drug delivery and increased stability of the incorporated drug, there are still some limitations. It has been observed that the incorporated drugs have a tendency to be expelled from the SLN during storage.[6] The inability of the SLN to retain loaded drugs is attributed to the highly-ordered crystalline lipid matrix that facilitates uncontrolled release from the nanoparticle. To overcome the problems associated with the SLN, nanostructured lipid carriers (NLCs) were developed.[7] The NLC is a second-generation SLN, consisting of solid and liquid lipid in proportions that prevent formation of perfect crystals.[8] Thus, loading of drugs into NLCs eliminates the disadvantages of SLNs by increasing drug-loading while preventing drug expulsion.[7]

Zerumbone is a natural compound isolated from essential volatile oil of rhizomes from the edible wild ginger, *Zingiber zerumbet* (L.) Smith.[9] Although zerumbone was recently shown to have several favorable pharmacologic properties, poor water solubility has limited its therapeutic use. The solubility of zerumbone can be improved by incorporation into an NLC. A physically stable zerumbone-loaded NLC (ZER-NLC) with up to 5% lipid content was developed using a high-pressure homogenization technique and characterized to be stable, relative small, and with a narrow size range and high zerumbone entrapment efficiency.[10,11] Several studies have shown that zerumbone has anticancer properties.[12] However, since this is the first zerumbone-loaded nanoparticle ever produced, the biological effect of zerumbone via a nanoparticle delivery system is not known. In this study, the objective was to determine the effect of a ZER-NLC on proliferation of an acute T-lymphoblastic leukemia (Jurkat) cell line.

Materials and methods

Leukemia cell line

A human acute T-lymphocyte leukemia (Jurkat) cell line was purchased from the American Type Culture Collection (Baltimore, MD, USA) and grown according to the recommended protocol.

Zerumbone-loaded NLC

Pure colorless zerumbone crystals were prepared from essential oil of fresh *Zingiber zerumbet* rhizomes extracted by steam distillation according to a method described earlier.[11] The ZER-NLC prepared by high-pressure homogenization were characterized by zetasizer, reverse phase high-performance liquid chromatography, transmission electron microscopy, wide angle x-ray diffraction, differential scanning colorimetry, and Franz diffusion cell analysis and shown to be physically stable, with a particle size of 52.68±0.1 nm, a zeta potential of −25.03±1.24 mV, and a polydispersity index of 0.29±0.0041 μm.[10,11]

Cytotoxicity of ZER-NLC toward human peripheral blood mononuclear cells

Human peripheral blood mononuclear cells were separated using a Vacutainer® (CPT™; BD, Franklin Lakes, NJ, USA) containing cell separation medium with sodium citrate following the instructions of the manufacturer. The cytotoxic effect of ZER-NLC on human peripheral blood mononuclear cells was determined at several concentrations (25, 50, and 100 μg/mL) after 24, 48, and 72 hours of incubation using the 3-[4,5-dimethylthiazol-2-yl]-2,5 diphenyl tetrazolium bromide (MTT) assay as previously described.[13] The assay was performed in triplicate and dimethyl sulfoxide (0.1% v/v; Sigma-Aldrich, St Louis, MO, USA) was used as the negative control.

Fluorescence microscopy

The effect of the ZER-NLC on the morphology of Jurkat cells was investigated using an acridine orange/propidium iodide double staining method according to the standard procedure described elsewhere[14] and examined under a fluorescence microscope (Leica, Tokyo, Japan).

Scanning and transmission electron microscopy

Jurkat cells were cultured with 5.39 μg/mL (half-maximal inhibitory concentration at 72 hours) of ZER-NLC, then incubated for 24, 48, and 72 hours, and processed for scanning electron microscopy and transmission electron microscopy according to a standard method. The specimens were viewed under a scanning electron microscope (64000; JEOL, Tokyo, Japan) at an accelerating voltage of 15–25 kV.

Sections on copper grids were stained and viewed under a transmission electron microscope (Phillips, Eindhoven, the Netherlands).

Annexin V-fluorescein isothiocyanate assay

Apoptosis of Jurkat cells was determined using an Annexin V-fluorescein isothiocyanate (FITC) kit (Sigma-Aldrich) according to the manufacturer's instructions without modifications, followed by flow cytometric analysis in a BD flow cytometer equipped with an argon laser (Cyan ADP; Dako Denmark A/P, Glostrup, Denmark) and with emitting excitation light at 488 nm. The data were analyzed using Summit version 4.3 software (Beckman Coulter, Inc., Brea, CA, USA).

Cell cycle analysis

Cell cycle analysis by means of flow cytometry was also done to provide evidence of cytotoxicity of the ZER-NLC toward Jurkat cells, according to a protocol described earlier but with minor modification.[15]

Tdt-mediated dUTP nick-end labeling assay

Apoptosis in Jurkat cells treated with the ZER-NLC was evaluated using the Tdt-mediated dUTP nick-end labeling (TUNEL) assay according to the manufacturer's protocol (DeadEnd™ fluorometric TUNEL system; Promega, Madison, WI, USA) and analyzed in a FACSCalibur flow cytometer (BD) equipped with an argon laser (BD).

Caspase-3, caspase-8, and caspase-9 assay

The activity of caspase-3, caspase-8, and caspase-9 in Jurkat cells treated with the ZER-NLC was determined spectrophotometrically using a commercial colorimetric assay kit (Genscript Corporation Inc, Piscataway, NJ, USA) according to the manufacturer's instructions.

Western blotting

Jurkat cells at a concentration of 1×10^6 cells/mL were treated with the ZER-NLC and lysed in radioimmunoprecipitation assay (RIPA) lysis buffer (Thermo Fisher Scientific, Waltham, MA, USA) containing a protease inhibitor cocktail (Sigma-Aldrich) according to the instructions of the manufacturer. Next, 25 μg of the protein was resolved on 10% sodium dodecyl sulfate polyacrylamide gel. A broad (11.0–240.0 kDa) prestained protein molecular weight ladder (GeneDirex, Inc., Las Vegas City, Nevada, USA) was used. After electrophoresis, the proteins were transferred to polyvinylidene difluoride membranes (Bio-Rad Laboratories, Hercules, CA, USA) and blocked with 5% nonfat dry milk in phosphate-buffered saline with 0.05% Tween 20 for 1 hour at room temperature. The membranes were probed with primary rabbit anti-Bcl-2, Bax, cytochrome c, poly (adenosine diphosphate-ribose) polymerase (PARP), or cyclin B1 antibody (Abcam, Cambridge, MA, USA) followed by horseradish peroxidase-conjugated secondary rabbit anti-goat antibody (Abcam, USA). The immunoreacted proteins were detected using a chemiluminescence system (ECL Western blot substrate; Abcam, Cambridge, UK). To ensure equal loading, the membranes were also probed with rabbit anti-β-actin antibody (Abcam, USA). The bands obtained were quantitated using Image J software (Bio Techniques, New York, NY, USA).

Statistical analysis

The experiments were done in triplicate and the results are expressed as the mean ± standard deviation. Statistical analysis was done using Statistical Package for the Social Sciences version 17 software (SPSS Inc, Chicago, IL, USA). The data were analyzed using post hoc comparison one-way analysis of variance, with means compared by Tukey's b test. Probability values of less than alpha 0.05 ($P<0.05$) were considered to be statistically significant.

Results and discussion

ZER-NLC inhibits proliferation of Jurkat cells

Chemopreventive agents have different effects on cancerous and normal cells. In the case of the ZER-NLC, there was no adverse effect on proliferation of human peripheral blood mononuclear cells at the dosages used and the periods of treatment (Figure 1), suggesting that it is not toxic to normal human peripheral blood mononuclear cells.

Our previous study showed that free zerumbone has strong inhibitory effects toward Jurkat cells in a time-dependent manner with a half-maximal inhibitory concentration of 12.5±0.1 μg/mL, 9.09±0.14 μg/mL, and 5.64±0.19 μg/mL after 24, 48, and 72 hours of incubation, respectively, while for the ZER-NLC the corresponding values were 11.87±0.17 μg/mL, 8.59±0.48 μg/mL, and 5.39±0.43 μg/mL, respectively. This suggests that the effect of ZER-NLC on Jurkat cells was similar to that of free zerumbone.[11]

Generally, the cytotoxic effect of drug-loaded nanoparticles occurs by adherence to the cell membrane, internalization and degradation, and intracellular release of the loaded drug. Since the NLC contains natural lipids, it is well tolerated by the organism. It is a prerequisite for human use that a loaded nanoparticle is of acceptable low toxicity. Since ZER-NLC

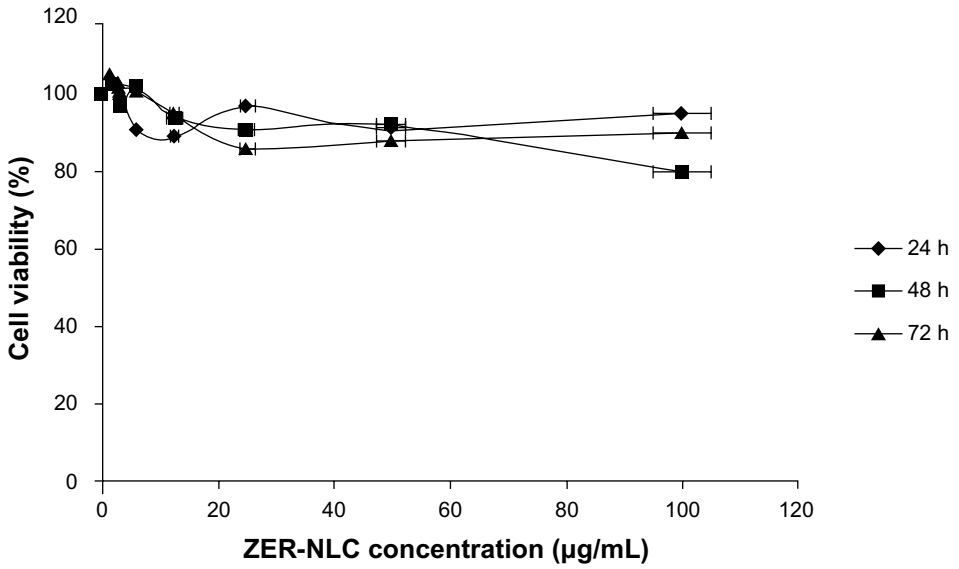

Figure 1 Effect of ZER-NLC on normal human peripheral blood mononuclear cells assessed by 3-[4,5-dimethylthiazol-2-yl]-2,5 diphenyl tetrazolium bromide (MTT) assay. The cells were treated for 24, 48, and 72 hours(h). The results are shown as the mean percentage of absorbance ± standard deviation of three separate experiments. No significant ($P>0.05$) decreases in cell viability were observed at any concentration.
Abbreviation: ZER-NLC, zerumbone-loaded nanostructured lipid carrier.

is intended for parenteral use, the potential toxic effect of the compound was assessed by in vitro and in vivo assays.[16] We demonstrated that the anticancer activity of zerumbone is not affected or impaired by incorporation into an NLC. Upon administration, zerumbone is immediately available to target cells, whereas the ZER-NLC needs to be internalized into cells via endocytosis or phagocytosis and degraded before zerumbone is released from the nanoparticles to produce an effect.[17,18] Considering that release of zerumbone from the nanoparticles can be by fractions, ie, according to the rate of nanoparticle degeneration, it is possible for the ZER-NLC to act upon target cells in a sustained manner. This would then perhaps allow ZER-NLC to be more effective than pure zerumbone in terms of prolonged anticancer activity.

Quantification of apoptosis using acridine orange/propidium iodide double staining

In this study, the apoptosis, necrosis, and viability of leukemic cells treated with ZER-NLC were investigated under a fluorescence microscope using acridine orange and propidium iodide stains (Figures 2 and S1). Late apoptotic cells were characterized by formation of orange-colored apoptotic bodies due to binding of acridine orange to denaturated DNA and chromatin condensation, whilst necrotic cells displayed a reddish-orange intact nucleus. Blebbing, chromatin condensation, and nuclear margination were noticed in the Jurkat cells after 48 hours of treatment, indicating that ZER-NLC induced apoptosis of these cells.

Ultrastructural changes in Jurkat cells treated with ZER-NLC

Scanning electron microscopy is a useful aid for observing morphologic changes in ZER-NLC-treated leukemic cells. In this study, distinct morphologic alterations in ZER-NLC-treated Jurkat cells were observed, as suggested by a cellular

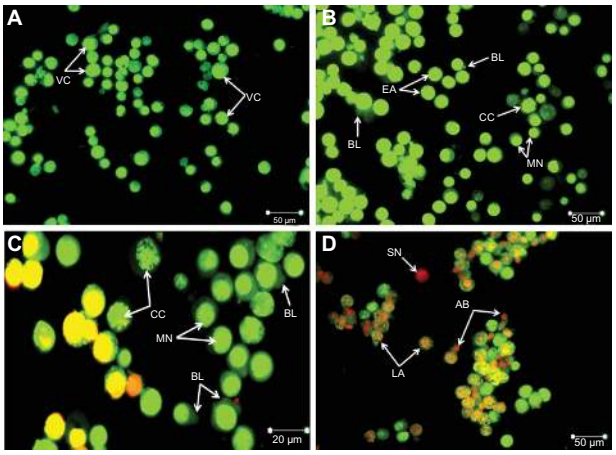

Figure 2 Fluorescent micrograph of acridine orange/propidium iodide double-stained Jurkat cells treated with the ZER-NLC. (**A**) Untreated cells showing a normal structure. (**B**) Early apoptosis of cells after 24 hours of treatment showing intercalated bright green staining with a marginated nucleus, chromatin condensation, and blebbing. (**C**) Blebbing, chromatin condensation, and nuclear margination after 48 hours of treatment. (**D**) Late apoptosis of cells after 72 hours of treatment showing reddish-orange staining with apoptotic body formation. Secondary necrotic cells displayed a reddish nucleus with an intact structure (400× magnification).
Abbreviations: VC, viable cells; EA, early apoptotic cells; CC, chromatin condensation; MN, marginated nucleus; BL, cell membrane blebbing; AB, apoptotic body; LA, late apoptotic cells; SN, secondary necrotic cell; ZER-NLC, zerumbone-loaded nanostructured lipid carrier.

morphology typical of apoptosis, including membrane blebbing and hole formation after 24 hours of treatment. Later, at 48 hours and 72 hours, the cells showed shrinkage and increased surface irregularities, with larger holes, cytoplasmic extensions, and formation of apoptotic bodies (Figures 3 and 4). These morphologic changes were time-related phenomena. In contrast, untreated normal Jurkat cells showed no morphologic changes and remained relatively round-shaped to oval-shaped, with the presence of microvilli. Under scanning electron microscopy, there was also evidence of membrane blebbing, cell shrinkage, formation of apoptotic bodies, dilated nuclear membranes, an increased nuclear to cytoplasm ratio, nuclear chromatin condensation and margination, swollen microvilli, cytoplasmic vacuolization, reduced cellular organelles, loss, rupture, and condensation of mitochondrial cristae with inclusion bodies, and formation of apoptotic micronuclei. All these morphologic changes are characteristic of apoptosis and are time-dependent. Untreated Jurkat cells showed a morphology and structure typical of the usual morphology of the cell line, ie, a round shape with a large nucleus and clear nucleoli, a normal double membrane nuclear envelope, uniformly distributed chromatin material, normal cytoplasm, and well developed cellular organelles. Further, the mitochondria of untreated control cells showed parallel and intact cristae. These results strongly suggest that the ZER-NLC has promising anticancer activity in human leukemic cells.

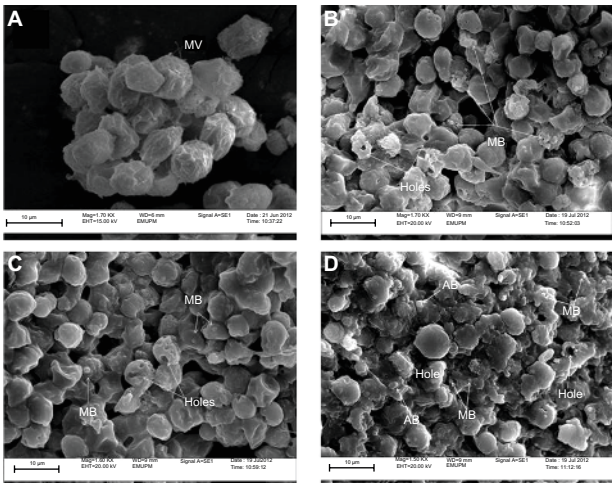

Figure 3 Ultrastructure of Jurkat cells treated with ZER-NLC. (**A**) Untreated control cells with typical cancer cell morphologic features with numerous MV. (**B**) Cells treated for 24 hours showing membrane blebbing and hole formation. (**C**) Cells treated for 48 hours showing cell shrinkage, increasing membrane blebbing, and hole formation. (**D**) Cells treated for 72 hours showing distinctive morphologic changes typical of apoptosis, including membrane blebbing and cell shrinkage with apoptotic body and hole formation.

Abbreviations: AB, apoptotic body; MB, membrane blebbing; MV, microvilli; ZER-NLC, zerumbone-loaded nanostructured lipid carrier; Mag, magnification; EMUPM, electron microscopy-university Putra Malaysia; EHT, extra high tension; WD, width.

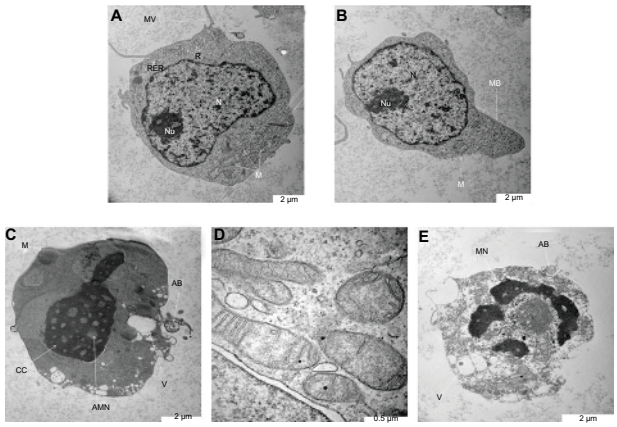

Figure 4 Ultrastructure of Jurkat cells treated with the zerumbone-loaded nanostructured lipid carrier. (**A**) Untreated control cells demonstrate a structure and morphology typical of leukemic cells. The nucleus (N) contains evenly distributed chromatin and a large nucleolus (Nu). Large and numerous mitochondria (M), rough endoplasmic reticulum (RER), ribosome (R), and typical microvilli (MV) are also seen. (**B**) Cells treated for 24 hours showing early-stage apoptosis characterized by membrane blebbing (MB) and a reduced number of cell organelles. (**C**) Cells treated for 48 hours showing mid-stage apoptosis characterized by chromatin condensation (CC), formation of apoptotic micronuclei (AMN), and apoptotic bodies (AB) with vacuolization (V). Loss, rupture, and condensation of mitochondria cristae in the Jurkat cells also occurred after 48 hours of treatment (**D**). (**E**) Cells treated for 72 hours showing late-stage apoptosis characterized by distinct morphologic changes, including cell shrinkage, increased cell granularity, nuclear margination (MN), AB and V.

Translocation of phosphatidylserine

Externalization of phosphatidylserine to the outer plasma membrane is a characteristic feature of apoptosis that can be detected via its high affinity for Annexin-V, a phospholipid-binding protein. Thus, apoptotic cells bound to fluorochrome-labeled Annexin-V can be visualized by fluorescence microscopy, flow cytometry, or determined by enzyme-linked immunosorbent assay fluorescence estimations.[19] In this study, after treatment with the ZER-NLC, the percentage of viable cells gradually decreased in a time-dependent manner, whilst the percentage of both early and late apoptotic cells gradually increased. With time, there was a significant ($P<0.5$) shift from early apoptosis to late apoptosis in the distribution of Jurkat cells (Figure 5 and Table S1). This observation confirms further that the ZER-NLC induces apoptosis in Jurkat cells, and that the effect is time-dependent.

Effect of ZER-NLC on cell cycle

We also determined the effect of the ZER-NLC on the Jurkat cell cycle. Jurkat cells were incubated with half-maximal inhibitory concentrations of ZER-NLC for 12, 24, 48, and 72 hours, and the cell cycle was determined by flow cytometry. The results show that the ZER-NLC induced depletion of the G1 phase of the Jurkat cell cycle with concomitant accumulation of the G2/M phase (Figure 6 and

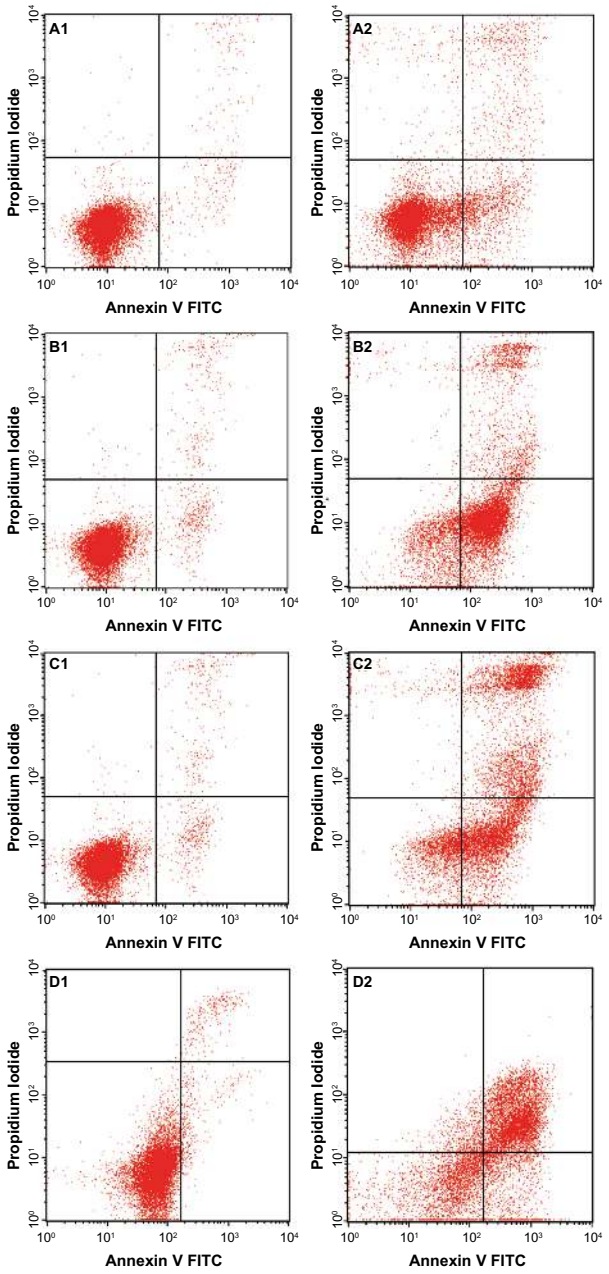

Figure 5 Flow cytometric analysis of Jurkat cells treated with the zerumbone-loaded nanostructured lipid carrier and after staining with FITC-conjugated Annexin V and propidium iodide. (**A1**–**D1**) Untreated Jurkat cell control at 6, 12, 24, and 48 hours, respectively. (**A2**–**D2**) Jurkat cells treated with the zerumbone-loaded nanostructured lipid carrier for 6, 12, 24, and 48 hours, respectively.
Abbreviation: FITC, fluorescein isothiocyanate.

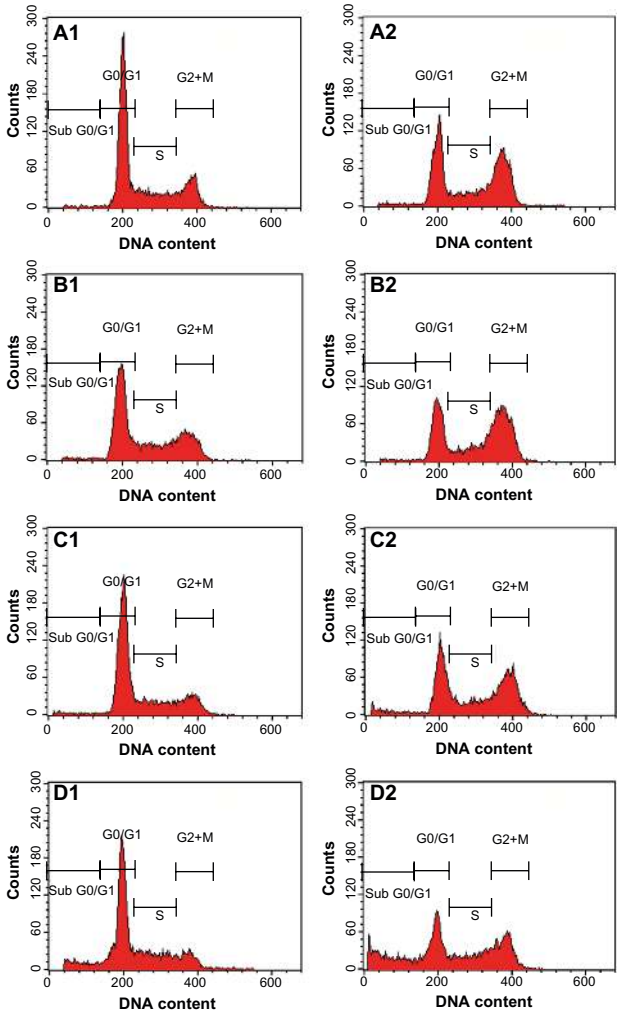

Figure 6 Analysis of the Jurkat cell cycle after treatment with the zerumbone-loaded nanostructured lipid carrier. The DNA content was analyzed by flow cytometry. (**A1**–**D1**) Untreated Jurkat control cells after 12, 24, 48, and 72 hours. (**A2**–**D2**) Jurkat cells treated with the zerumbone-loaded nanostructured lipid carrier for 12, 24, 48, and 72 hours. G0/G1, G2/M, and S are cell phases, and sub-G1 DNA content refers to apoptotic cells.

Table S2). There was also significant ($P<0.05$) G2/M arrest at 12–72 hours of treatment (Figure S2). The dysregulation in cell cycle progression initiated by activation of growth-stimulating oncogenes is one of the primary characteristics of cancer cells. Cell cycle progression is tightly controlled by regulation of expression and activity of cyclin/cyclin-dependent kinase complexes. In cell cycle dysregulation, there is overexpression of cell cycle growth promoting factors such as cyclin B1 and cyclin/cyclin-dependent kinase typical of tumorigenesis. Many dietary compounds, including curcumin, resveratrol, genistein, apigenin, silibinin, and ginger, have been shown to dysregulate the cycle of cancer cells.[20] This is also true for the ZER-NLC, whereby these loaded nanoparticles induced G2/M arrest and apoptosis in Jurkat cells, probably by inhibition of cyclin/cyclin-dependent kinase.

Effect of ZER-NLC on DNA fragmentation

Generally, apoptotic endonucleases degrade chromosomal DNA during apoptosis. The TUNEL assay was employed to determine whether or not the ZER-NLC induces DNA fragmentation in Jurkat cells. Our results show that the ZER-NLC significantly ($P<0.5$) increased DNA fragmentation in Jurkat

cells and this effect increased with duration of treatment (Figure 7 and Table S3).

Effect of ZER-NLC on caspase activity

Caspase-3 is the hallmark enzyme of apoptosis, and is required for DNA fragmentation and most morphologic changes related to apoptosis.[21] Caspase-9 is an enzyme in the mitochondrial intrinsic pathway, and precedes caspase-3.[22] In this study, the activity of three caspases was determined in ZER-NLC-treated Jurkat cells in vitro (Figure 8 and Table S4). The ZER-NLC significantly ($P<0.5$) stimulated caspase-3 and caspase-9 to more than a one-fold increase in activity in a dose-dependent manner, while producing a lesser effect on caspase-8 activity. The results suggest that the apoptogenic effect of ZER-NLC on Jurkat cells is via the intrinsic mitochondrial pathway.

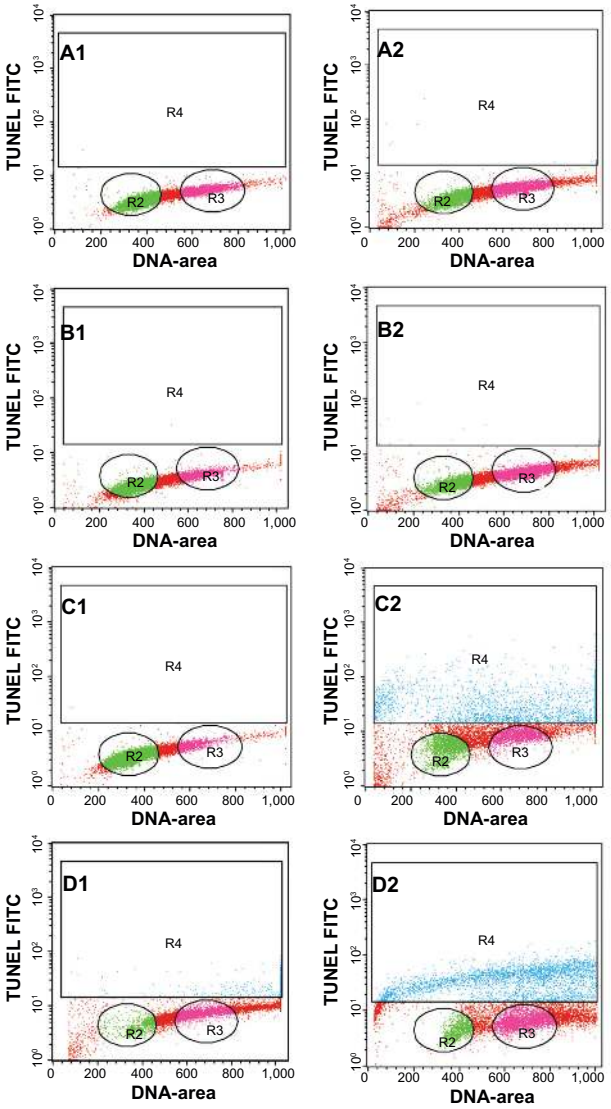

Figure 7 Apoptosis of Jurkat cells treated with the zerumbone-loaded nanostructured lipid carrier as determined by flow cytometry after staining with rTdT. (**A1**–**D1**) Untreated Jurkat cells at 12, 24, 48, and 72 hours. (**A2**–**D2**) Jurkat cells treated for 12, 24, 48, and 72 hours. Cells in the lower quadrant (R2 and R3) are nonapoptotic and cells in the upper quadrant (R4) are apoptotic.
Abbreviations: TUNEL, Tdt-mediated dUTP nick-end labeling; FITC, fluorescein isothiocyanate.

Western blotting

The Western blot assay was used to investigate the expression of apoptotic proteins and the mechanism by which the ZER-NLC induces apoptosis in Jurkat cells. We found that ZER-NLC significantly ($P<0.05$) downregulated Bcl-2 protein and upregulated Bax protein. Cytochrome c protein gradually increased in the cytosol, in parallel with the duration of treatment with ZER-NLC. Thus, release of cytochrome c induced activation of caspase-9 and caspase-3 which subsequently cleaved 116 kDa PARP protein into an 85 kDa fragment. The expression of cyclin B1 also decreased with duration of treatment (Table S5). β-actin showed equal intensity bands, confirming the presence of an equal protein concentration in all loaded samples (Figure 9A). Significant ($P<0.05$) differences in relative expression levels for all proteins were found between treated and untreated control cells (Figure 9B).

Mammalian cells have two main apoptotic pathways, ie, the extrinsic and intrinsic pathways. The extrinsic pathway is initiated by extrinsic ligand binding to death receptors, such as Fas cluster of differentiation 95 (CD95), which in turn activate caspase-8. The intrinsic mitochondrial pathway is regulated by Bcl-2 family proteins. The Bcl-2 family comprise the major apoptotic proteins governing mitochondrial membrane permeability and can be either proapoptotic, such as Bax, or antiapoptotic, such as Bcl-2.[23,24] Downregulation of Bcl-2 could lead to permeabilization of the outer mitochondrial membrane and facilitate the release of mitochondrial cytochrome c into the cytoplasm. Cytochrome c binds to deoxyadenosine triphosphate and apoptotic protease activating factor 1 to form a multiprotein complex known as the apoptosome, which functions to activate caspase-9 and thus to execute the apoptotic process. Apoptosome triggers activation of caspase-3, which cleaves its substrate, PARP, a nuclear enzyme important for DNA repair.[25] Our results suggest that zerumbone initiates apoptosis in Jurkat cells via the mitochondrial intrinsic apoptotic pathway (Figure 10).

To gain a better understanding of the mechanism underlying G2/M arrest in ZER-NLC treated Jurkat cells, we examined the levels of protein that regulate G2/M transition, such as cyclin B1 protein. G2/M arrest is usually dependent on a checkpoint kinase 1-associated signaling pathway leading to inhibition of cyclin B1/cell division control protein 2 activity. Our results show that the ZER-NLC downregulates this protein in a time-dependent manner, suggesting that it induced phosphorylation of Cdc2 at the threonine (Thr)14 and

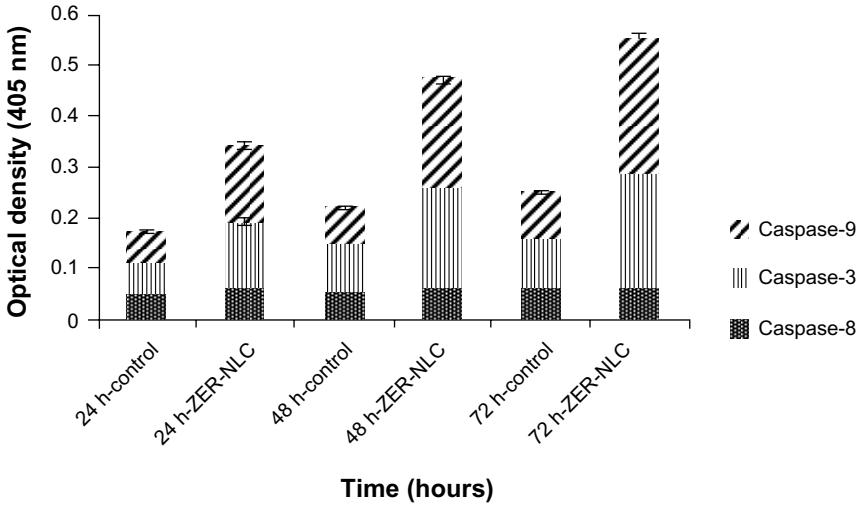

Figure 8 Caspase activity in untreated control Jurkat cells and Jurkat cells treated with the ZER-NLC at 24, 48, and 72 hours(h). The results show statistically significant ($P<0.05$) differences in caspase-3 and caspase-9 activity between untreated and treated cells, but no statistically significant ($P>0.05$) activity for caspase-8.
Abbreviation: ZER-NLC, zerumbone-loaded nanostructured lipid carrier.

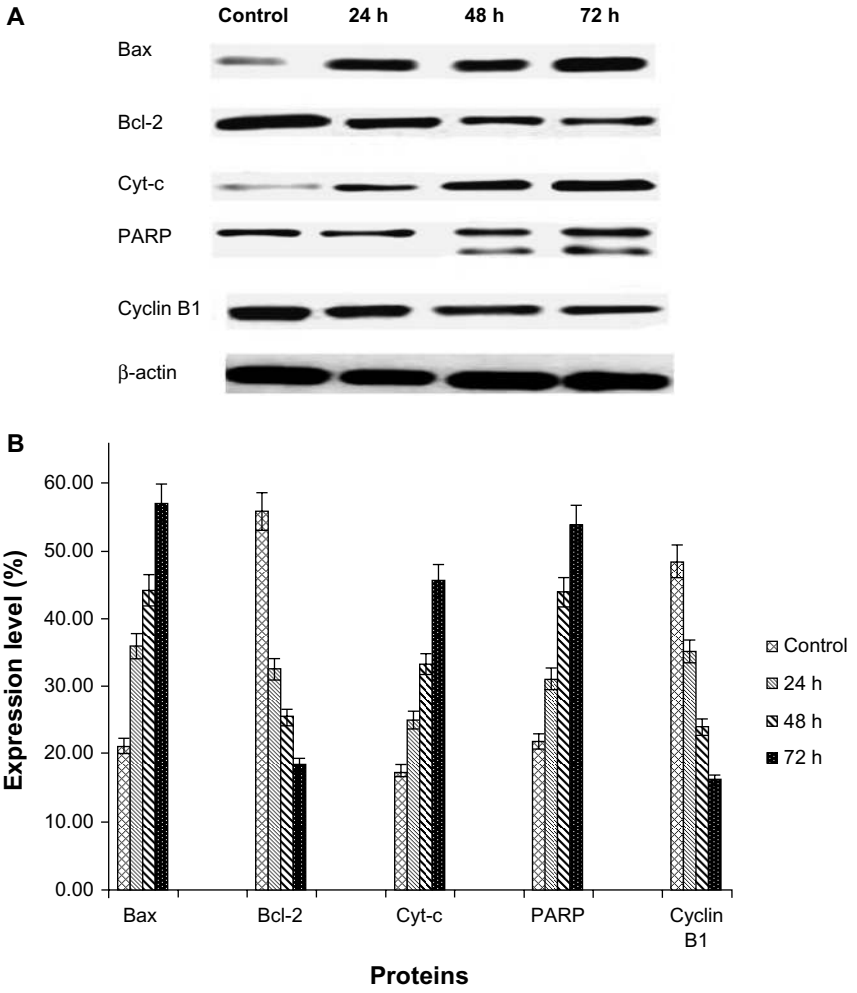

Figure 9 (**A**) Western blots showing the effect of the zerumbone-loaded nanostructured lipid carrier on levels of cell cycle proteins regulating apoptosis in Jurkat cells after 24, 48, and 72 hours(h). B-actin was used as the loading control. (**B**) Western blotting analysis of the zerumbone-loaded nanostructured lipid carrier in Jurkat cells. The level of each protein was measured and normalized to β-actin. The values are shown as the mean ± standard deviation percentage of three independent experiments. Statistically significant differences ($P<0.05$) were found between treated cells and control cells in each group.
Abbreviations: Cyt-c, cytochrome c; Bcl-2, B cell lymphoma 2; Bax, Bcl-2 associated X protein; PARP, poly(adenosine diphosphate-ribose) polymerase; β-actin, Beta actin.

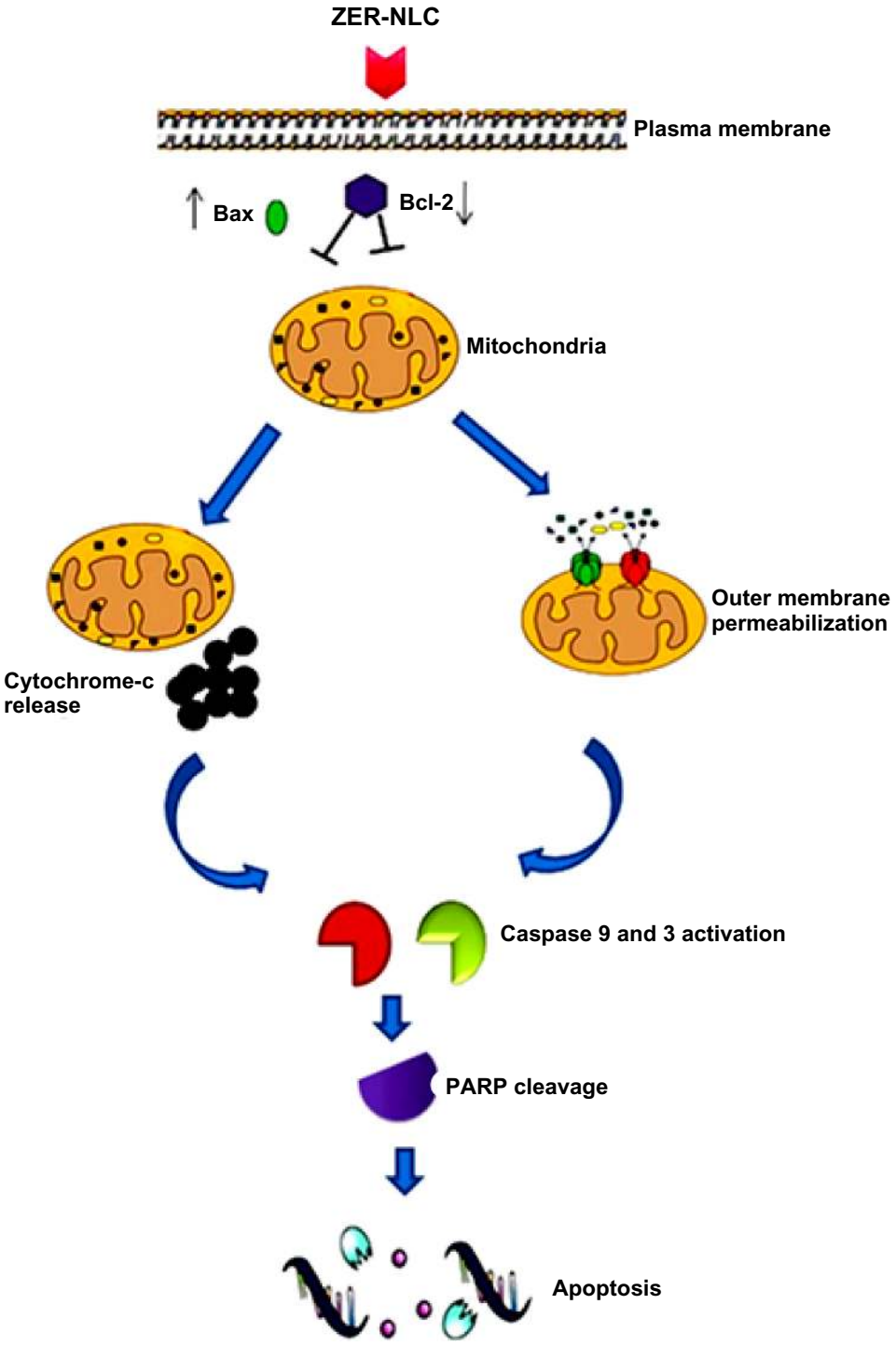

Figure 10 Hypothetical diagram demonstrating possible apoptotic effects of the ZER-NLC in Jurkat cells in vitro.
Abbreviations: ZER-NLC, zerumbone-loaded nanostructured lipid carrier; Bcl-2, B cell lymphoma 2; Bax, Bcl-2 associated X protein; PARP, poly(adenosine diphosphate-ribose) polymerase.

tyrosine15 residues and Cdc25C at the Thr48 residue before entering into mitosis and thereby inactivating cyclin B1.[26]

Conclusion

This study provides clear and substantial evidence that the ZER-NLC is a potentially effective drug delivery system for the treatment of leukemia. The anticancer effect of ZER-NLC in an acute human lymphoblastic leukemia cell line occurs via induction of the mitochondrial pathway of apoptosis and the effect is both dose-dependent and time-dependent. Loading of zerumbone into an NLC did not diminish the anticancer effect of zerumbone. The current study also shows for the

first time, that the NLC can be used as a carrier for delivery of zerumbone in the treatment of cancer. Thus, the ZER-NLC is safe for parenteral use and can be developed into an innovative regimen for the treatment of cancer.

Acknowledgments

We would like to acknowledge the Institute of Bioscience, Faculty of Biotechnology, and the Faculty of Veterinary Medicine, Universiti Putra Malaysia, for providing their facilities and technical support. Special thanks are extended to the Ministry of Science, Technology, and Innovation, Malaysia, for funding this project.

Disclosure

The authors report no conflicts of interest in this work.

References

1. Junghanns JU, Müller RH. Nanocrystal technology, drug delivery and clinical applications. *Int J Nanomedicine*. 2008;3:295–309.
2. Al Haj NA, Abdullah R, Ibrahim S, Bustamam A. Tamoxifen drug loading solid lipid nanoparticles prepared by hot high pressure homogenization techniques. *Am J Pharmacol Toxicol*. 2008;3:219–224.
3. Selvamuthukumar S, Velmurugan R. Nanostructured lipid carriers. *Lipids Health Dis*. 2012;11:159.
4. How CW, Abdullah R, Abbasalipourkabir R. Physicochemical properties of nanostructured lipid carriers as colloidal carrier system stabilized with polysorbate 20 and polysorbate 80. *Afr J Biotechnol*. 2011;10:1684–1689.
5. De Jong WH, Borm PJA. Drug delivery and nanoparticles: applications and hazards. *Int J Nanomedicine*. 2008;3:133–149.
6. Abbasalipourkabir R, Salehzada A, Rasedee A. Solid lipid nanoparticles as new drug delivery system. *Indian J Pharm Sci*. 2011;2:252–261.
7. Meghana SK, Krunal KV, Ashok VB, Pravin DC. Solid lipid nanoparticles and nanostructured lipid carriers. *International Journal of Pharmacy and Biological Sciences*. 2012;2:681–691.
8. Fathi M, Varshosaz J, Mohebbi M, Shahidi F. Hesperetin-loaded solid lipid nanoparticles and nanostructure lipid carriers for food fortification: preparation, characterization, and modeling. *Food and Bioprocess Technology*. 2012;6:1464–1475.
9. Kitayama T. Attractive reactivity of a natural product, zerumbone. *Biosci Biotechnol Biochem*. 2011;75:199–207.
10. Rasedee A, Heshu SR, Ahmad Bustamam A, How CW, Swee KY. A composition for treating leukaemia. Malaysian Patent Application. 2013; PI2013700213.
11. Rahman HS, Rasedee A, How CW, et al. Zerumbone-loaded nanostructured lipid carrier: preparation, characterization, and antileukemic effect. *Int J Nanomedicine*. 2013;8:2769–2781.
12. Prasannan R, Kalesh KA, Shanmugam MK, et al. Key cell signalling pathways modulated by zerumbone: role in the prevention and treatment of cancer. *Biochem Pharmacol*. 2012;84:1268–1276.
13. Miyoshi N, Nakamura Y, Ueda Y, et al. Dietary ginger constituents, galanals A and B, are potent apoptosis inducers in human T lymphoma Jurkat cells. *Cancer Lett*. 2003;199:113–119.
14. Anassamy T, Abdul AB, Sukari MA, et al. A phenylbutenoid dimer, cis-3-(3′, 4′-dimethoxyphenyl)-4-[(E)-3‴, 4‴-dimethoxystyryl] cyclohex-1-ene, exhibits apoptogenic properties in T-acute lymphoblastic leukemia cells via induction of p53-independent mitochondrial signalling pathway. *Evid Based Complement Alternat Med*. 2013;2013:939810.
15. Syam S, Abdul AB, Sukari MA, Mohan S, Abdelwahab SI, Wah TS. The growth suppressing effects of girinimbine on HepG2 involve induction of apoptosis and cell cycle arrest. *Molecules*. 2011;16:7155–7170.
16. Su X, Fricke J, Kavanagh DG, Irvine DJ. In vitro and in vivo mRNA delivery using lipid-enveloped pH-responsive polymer nanoparticles. *Mol Pharm*. 2011;8:774–787.
17. Xin H, Chen L, Gu J, et al. Enhanced anti-glioblastoma efficacy by PTX-loaded PEGylated poly (ε-caprolactone) nanoparticles: in vitro and in vivo evaluation. *Int J Pharm*. 2010;402:238–347.
18. Chen H, Kim S, Li L, Wang S, Park K, Cheng J-X. Release of hydrophobic molecules from polymer micelles into cell membranes revealed by Förster resonance energy transfer imaging. *Proc Natl Acad Sci U S A*. 2008;105:6596–6601.
19. Schiller M, Bekeredjian-Ding I, Heyder P, Blank N, Ho AD, Lorenz H-M. Autoantigens are translocated into small apoptotic bodies during early stages of apoptosis. *Cell Death Differ*. 2007;15:183–191.
20. Aggarwal BB, Shishodia S. Molecular targets of dietary agents for prevention and therapy of cancer. *Biochem Pharmacol*. 2006;71:1397–1421.
21. Jänicke RU, Sprengart ML, Wati MR, Porter AG. Caspase-3 is required for DNA fragmentation and morphological changes associated with apoptosis. *J Biol Chem*. 1998;273:9357–9360.
22. Brentnall M, Rodriguez-Menocal L, De Guevara RL, Cepero E, Boise LH. Caspase-9, caspase-3 and caspase-7 have distinct roles during intrinsic apoptosis. *BMC Cell Biol*. 2013;14:32.
23. Brunelle JK, Letai A. Control of mitochondrial apoptosis by the Bcl-2 family. *J Cell Sci*. 2009;122:437–441.
24. Rahman MA, Sultan MT, Islam MR. Apoptosis and cancer: insights molecular mechanisms and treatments. *Int J Biomol Biomed*. 2012;2:1–16.
25. Elmore S. Apoptosis: a review of programmed cell death. *Toxicol Pathol*. 2007;35:495–516.
26. Xian M, Ito K, Nakazato T, et al. Zerumbone, a bioactive sesquiterpene, induces G2/M cell cycle arrest and apoptosis in leukemia cells via a Fas and mitochondria mediated pathway. *Cancer Sci*. 2007;98:118–126.

Supplementary data

Table S1 Flow cytometric analysis of Annexin V-FITC in Jurkat cells after treatment with ZER-NLC

Cell condition	Cells (%)							
	6 hours		12 hours		24 hours		48 hours	
	Control	ZER-NLC	Control	ZER-NLC	Control	ZER-NLC	Control	ZER-NLC
Viable cells	96.93±0.188	79.2±0.16	96.39±0.25	21.71±0.66	93.88±0.16	15.48±0.73	93.16±0.98	28.62±0.94
Early apoptosis	1.67±0.11	12.34±0.51*	1.85±0.07	63.08±0.48*	3.45±0.11	21.37±0.42*	3.91±0.54	12.15±0.40*
Late apoptosis/ necrosis	1.39±0.14	8.45±0.65**	1.76±0.2	15.19±0.12**	2.66±0.11	63.14±0.58**	2.92±0.44	59.34±1.10**

Notes: Values are expressed as the mean ± standard deviation of three different experiments. The data were analyzed using post hoc comparison test-one way analysis of variance, and the means were compared by Tukey's b test. *Significant ($P<0.05$) increase in early apoptotic cells in ZER-NLC-treated group versus untreated control. **Significant ($P<0.05$) increase in late apoptotic/necrotic cells in ZER-NLC-treated group versus untreated control.
Abbreviations: FITC, fluorescein isothiocyanate; ZER-NLC, zerumbone-loaded nanostructured lipid carrier.

Table S2 Flow cytometric analysis of Jurkat cell cycle after treatment with ZER-NLC

Cell cycle phase	Cells (%)							
	12 hours		24 hours		48 hours		72 hours	
	Control	ZER-NLC	Control	ZER-NLC	Control	ZER-NLC	Control	ZER-NLC
G0/G1	59.81±0.82	40.44±0.58	52.81±0.68	34.09±0.5	62.73±0.57	38.28±0.32	58.7±0.59	32.42±0.83
G2/M	18.38±0.53	35.46±0.49*	21.43±0.84	40.14±0.75*	15.36±0.55	34.91±1.22*	10.64±0.31	24.59±2.5*
S	21.51±0.47	22.83±0.08	24.79±0.33	24.46±0.35	19.81±0.32	21.83±0.5	21.75±0.69	21.45±1.2
SubG0/G1	0.81±0.07	1.39±0.06	1.56±0.09	1.99±0.64	2.47±0.24	5.52±0.47	9.27±0.67	22.12±0.76

Notes: Cells were stained with propidium iodide and incubated at 37°C for 24, 48, and 72 hours. Values are expressed as the mean ± standard deviation of three different experiments. The data were analyzed using post hoc comparison test-one way analysis of variance, and the means were compared by Tukey's b test. *Significant ($P<0.05$) increase in cells in G2/M phase in ZER-NLC-treated group versus untreated control.
Abbreviation: ZER-NLC, zerumbone-loaded nanostructured lipid carrier.

Table S3 TUNEL flow cytometric analysis of Jurkat cells treated with ZER-NLC

Cell condition	Cells (%)					
	24 hours		48 hours		72 hours	
	Control	ZER-NLC	Control	ZER-NLC	Control	ZER-NLC
Viable	96.63±0.4	77.75±0.09	97.63±0.21	68.97±0.7	95.68±0.24	60.31±1.07
Apoptotic	3.36±0.3	22.73±0.09*	2.36±0.5	31.19±0.7*	4.32±0.28	39.68±1.1*

Notes: Values are expressed as the mean ± standard deviation of three different experiments. The data were analyzed using post hoc comparison test-one way analysis of variance, with means compared by the Tukey's b test. *Significant ($P<0.05$) increase in apoptotic cells in ZER-NLC-treated group versus untreated control.
Abbreviations: TUNEL, Tdt-mediated dUTP nick-end labeling; ZER-NLC, zerumbone-loaded nanostructured lipid carrier.

Table S4 Spectrophotometric analysis of Jurkat cell caspase activity after treatment with ZER-NLC

Caspases	Cells (%)					
	24 hours		48 hours		72 hours	
	Control	ZER-NLC	Control	ZER-NLC	Control	ZER-NLC
Caspase-8	0.05±0.01	0.058±0.003	0.056±0.004	0.063±0.003	0.061±0.003	0.068±0.003
Caspase-3	0.06±0.003	0.13±0.01*	0.09±0.003	0.199±0.007*	0.1±0.1	0.221±0.01*
Caspase-9	0.065±0.001	0.151±0.016*	0.071±0.002	0.211±0.012*	0.086±0.001	0.261±0.011*

Notes: Values are expressed as the mean ± standard deviation of three different experiments. The data were analyzed using post hoc comparison test-one way analysis of variance, with means compared by Tukey's b test. *Significant ($P<0.05$) increase in caspase activity in the ZER-NLC-treated group versus untreated control.
Abbreviation: ZER-NLC, zerumbone-loaded nanostructured lipid carrier.

Table S5 Western blot analysis of protein transcription in ZER-NLC-treated Jurkat cells

Proteins	Control	24 hours	48 hours	72 hours
Protein transcription level (%)				
Bax	21.29	36.11*	44.32*	57.19*
Bcl-2	55.90	32.75**	25.54**	18.55**
Cyt-c	17.61	25.23*	33.45*	45.78*
PARP	22.02	31.20*	43.98*	54.11*
Cyclin B1	48.54	35.23**	24.14**	16.34**

Notes: Values are expressed as the mean ± standard deviation of three different experiments. The data were analyzed using post hoc comparison test-one way analysis of variance, with means compared by Tukey's b test. *Significant ($P<0.05$) upregulation of protein in the ZER-NLC-treated group versus untreated control. **Significant ($P<0.05$) downregulation of protein in ZER-NLC-treated group versus untreated control.

Abbreviations: PARP, poly(adenosine diphosphate-ribose) polymerase; ZER-NLC, zerumbone-loaded nanostructured lipid carrier; Bcl-2, B cell lymphoma 2; Bax, Bcl-2 associated X protein; Cyt-c, cytochrome c.

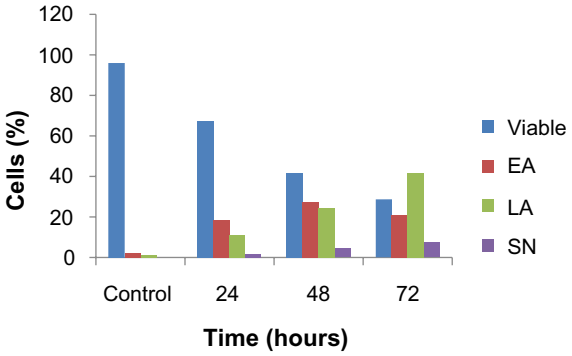

Figure S1 Percentages of viable, early apoptotic, late apoptotic, and secondary necrotic cells after treatment with the ZER-NLC for 24, 48, and 72 hours using the acridine orange/propidium iodide double-staining test. Jurkat cell death via apoptosis increased significantly ($P<0.05$) in a time-dependent manner, but no significant difference ($P>0.05$) was observed in the necrotic cell count.

Abbreviations: EA, early apoptosis; LA, late apoptosis; SN, secondary necrosis; ZER-NLC, zerumbone-loaded nanostructured lipid carrier.

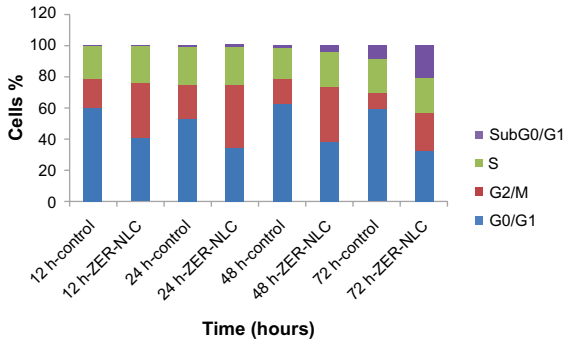

Figure S2 Profile of the Jurkat cell cycle in the presence of the ZER-NLC suspension. After 12, 24, 48, and 72 hours(h) of incubation with the ZER-NLC, the DNA content was evaluated with propidium iodide and acridine orange staining, and fluorescence was measured and then analyzed. The values are shown as the mean ± standard deviation percentage of three independent experiments.

Abbreviation: ZER-NLC, zerumbone-loaded nanostructured lipid carrier.